

## Comparative Studies on the Structure and Stability of Fluorescent Proteins EGFP, zFP506, mRFP1, “dimer2”, and DsRed1<sup>†</sup>

Olesia V. Stepanenko,<sup>‡</sup> Vladislav V. Verkhusha,<sup>§</sup> Vasili I. Kazakov,<sup>‡</sup> Michail M. Shavlovsky,<sup>||</sup>  
Irina M. Kuznetsova,<sup>‡</sup> Vladimir N. Uversky,<sup>\*,†,⊕,+</sup> and Konstantin K. Turoverov<sup>\*,‡</sup>

*Institute of Cytology, Russian Academy of Sciences, St. Petersburg 194064, Russia, Department of Pharmacology, University of Colorado Health Sciences Center, Denver, Colorado 80262, Institute of Experimental Medicine, Russian Academy of Medical Sciences, St. Petersburg 197376, Russia, Institute for Biological Instrumentation, Russian Academy of Sciences, Pushchino 142290, Moscow Region, Russia, Department of Biochemistry and Molecular Biology, University of Indianapolis-Purdue University at Indianapolis, School of Medicine, 635 Barnhill Drive, Indianapolis, Indiana 46202, and Molecular Kinetics, Inc., 6201 La Pas Trail, Suite 160, Indianapolis, Indiana 46268*

Received June 18, 2004; Revised Manuscript Received September 20, 2004

**ABSTRACT:** To obtain more information about the structural properties and conformational stabilities of GFP-like fluorescent proteins, we have undertaken a systematic analysis of series of green and red fluorescent proteins with different association states. The list of studied proteins includes EGFP (green monomer), zFP506 (green tetramer), mRFP1 (red monomer), “dimer2” (red dimer), and DsRed1 (red tetramer). Fluorescent and absorbance parameters, near-UV and visible CD spectra, the accessibility of the chromophores and tryptophans to acrylamide quenching, and the resistance of these proteins to the guanidine hydrochloride unfolding and kinetics of the approaching of the unfolding equilibrium have been compared. Tetrameric zFP506 was shown to be dramatically more stable than the EGFP monomer, assuming that association might contribute to the protein conformational stability. This assumption is most likely valid even though the sequences of GFP and zFP506 are only ~25% identical. Interestingly, red FPs possessed comparable conformational stabilities, where monomeric mRFP1 was the most stable species under the equilibrium conditions, whereas the tetrameric DsRed1 possessed the slowest unfolding kinetics. Furthermore, EGFP is shown to be considerably less stable than mRFP1, whereas tetrameric zFP506 is the most stable species analyzed in this study. This means that the quaternary structure, being an important stabilizing factor, does not represent the only circumstance dictating the dramatic variations between fluorescent proteins in their conformational stabilities.

Fluorescent bioimaging of single molecules, intact organelles, live cells, and whole organisms has become an invaluable approach in the fields of biochemistry, biotechnology, and cell and developmental biology (1). Cloning of green fluorescent protein (GFP)<sup>1</sup> from the jellyfish *Aequorea victoria* (class Hydrozoa) (2) and the subsequent creation of wavelength-shifted and enhanced mutants such as EBFP,

ECFP, EGFP (3–5), and EYFP (6) have made enormous impacts on biological research. Further crucial breakthroughs have come with recent cloning of novel GFP-like green, yellow, and red fluorescent proteins (FPs) (7–10) and nonfluorescent chromoproteins (CPs) from class Anthozoa (10–13). In fact, the discovery of a red GFP-like protein, DsRed1, from corallimorph *Discosoma* sp. (7) and development of its improved mutants, DsRed-Timer (14), DsRed2 (15), and fast-maturing DsRed-Express (16), have significantly increased the range of FP applications, including multicolor protein tagging (17), intracellular reporting (18), and resonance energy transfer (19). Overall, GFP-like proteins are a fast-growing family of homologous 25–30 kDa polypeptides that currently consists of ~140 cloned genes from both Cnidaria and Bilateria species (20). It is clear that understanding the relationship between the structure and spectral properties of FPs is of great scientific and practical interest. However, despite the abundance of available sequences, at present it is difficult to determine which amino acid positions are responsible for particular types of

<sup>†</sup> This work was supported in part by Grants AA13489(INIA) from the National Institute on Alcohol Abuse and Alcoholism and GM070358 from the National Institute of General Medical Sciences (to V.V.V.), the Russian Academy of Sciences for the “Molecular and Cellular Biology” program (to K.K.T. and V.N.U.), the Russian Academy of Sciences for the “Fundamental Science to Medicine” program (to V.N.U.), RFFI Grant 04-04-49290 (I.M.K.), and INTAS Grant 2001–2347 (to V.N.U., M.M.Sh., and K.K.T.).

\* To whom correspondence should be addressed. V.N.U.: Department of Biochemistry and Molecular Biology, University of Indianapolis-Purdue University at Indianapolis, School of Medicine, 635 Barnhill Dr., MS 4021, Indianapolis, IN 46202; fax, (317) 278-4686; phone, (317) 278-9194; e-mail, vversky@iupui.edu. K.K.T.: Institute of Cytology, Russian Academy of Sciences, St. Petersburg 194064, Russia; phone, 011-7-812-247-1829; fax, 011-7-812-247-0341; e-mail, kkt@mail.cytspb.rssi.ru.

<sup>‡</sup> Institute of Cytology, Russian Academy of Sciences.

<sup>§</sup> University of Colorado Health Sciences Center.

<sup>||</sup> Russian Academy of Medical Sciences.

<sup>†</sup> Institute for Biological Instrumentation, Russian Academy of Sciences.

<sup>⊕</sup> University of Indianapolis-Purdue University at Indianapolis.

<sup>+</sup> Molecular Kinetics, Inc.

<sup>1</sup> Abbreviations: GFP, green fluorescent protein; FP, fluorescent protein; CP, nonfluorescent chromoprotein; RBFP, enhanced blue FP; ECFP, enhanced cyan FP; EGFP, enhanced green FP; EYFP, enhanced yellow FP; DsRed1, red FP; zFP506, tetrameric GFP; mRFP1, monomeric red FP; dimer2, dimeric red FP; GdmCl, guanidine hydrochloride; CD, circular dichroism; UV, ultraviolet; vis, visible; FRET, fluorescence resonance energy transfer.

spectra. The only conclusive observation could be extracted from the analysis of available three-dimensional structures for FPs: the majority of positions responsible for the color change must be located near the chromophore.

GFP is a globular protein consisting of 238 amino acid residues (21). Crystallographic structures resolved for the wild-type GFP and its enhanced mutants (ECFP, 1C4F.ent, and EYFP) revealed that these proteins resemble an 11-stranded  $\beta$ -can wrapped around a single central helix in the middle of which is the chromophore (6, 22, 23). The cylinder has a diameter of  $\sim 30$  Å and a length of  $\sim 40$  Å (23). Being an important reporter for monitoring gene expression and protein localization in a variety of cells and organisms, wild-type GFP isolated from the jellyfish *A. victoria* has several undesirable properties, including low fluorescent intensity when excited by blue light, a lag in the development of fluorescence after protein synthesis, and poor expression in several mammalian cell types (24–27). To improve the spectral properties of GFP, a unique GFP variant (EGFP) has been constructed, which contained chromophore mutations (F64L/S65T mutant of GFP) that made the protein 35 times brighter than wild-type GFP (28). It has been shown that both GFP and EGFP are highly conformationally stable under a variety of conditions, including a treatment with detergents (29, 30), proteases (31), GdmCl (32, 33), and temperature (33, 34).

Interestingly, like GFP, the monomer of DsRed1 folds into a  $\beta$ -can (35). However, both sedimentation (36, 37) and crystallographic studies (35) have revealed that DsRed1 forms a tight tetramer with a nanomolar association constant (37). Among  $\sim 140$  distinct GFP-like proteins cloned to date (22), many have been shown to be characterized by obligate tetrameric structures (15). However, neither structural consequences nor the functional roles of this oligomerization are known as yet. Recently, conformational stabilities of EGFP and DsRed1 have been compared both *in vitro* and *in vivo* (33). It has been shown that the apparent rate constants of thermal and GdmCl-induced denaturation were several orders of magnitude lower for DsRed1 than for EGFP. Furthermore, several times longer lifetimes of DsRed1 versus EGFP were observed in cultured cells and in embryos. This remarkable conformational stability of DsRed1 under all the conditions that were studied was attributed to its tetrameric organization (33). The current work is aimed at checking the assumption about the crucial role of the oligomeric state in the conformational stability of FPs. To this end, a comparative analysis of several FPs with different degrees of oligomerization has been performed with respect to their stability toward the GdmCl-induced unfolding. The list of studied proteins includes EGFP (green monomer), zFP506 (green tetramer), mRFP1 (red monomer), “dimer2” (red dimer), and DsRed1 (red tetramer). The brief description of the proteins of interest is presented below.

To prevent red FP oligomerization, the monomer interfaces in the DsRed1 tetramer were modified by the insertion of positively charged arginines, which initially crippled the protein, but red fluorescence was then rescued by random and directed mutagenesis (38). The final monomeric mRFP1 mutant contains 33 mutations, of which 13 are internal to the  $\beta$ -barrel, three are in the short N-terminus, 13 are interface mutations, and four are in positions where the exact effects on structure and function are unknown. Although

mRFP1 has a 1.3 times lower extinction coefficient and a 3.2 times lower quantum yield, it acquires red fluorescence more than 10 times faster than DsRed1, being approximately as bright as DsRed1 in living cells (38).

The dimeric form of red FP, dimer2 (38), is a result of coupled site-directed and random mutagenesis of an engineered fast-maturing tetrameric variant of DsRed, known as T1 (16). The final variant contains 17 substitutions, eight of which are internal to the  $\beta$ -barrel (N42Q, V44A, V71A, F118L, K163Q, S179T, S197T, and T217S), three of which are the aggregation-reducing mutations, found in T1 (R2A, K5E, and N6D) (16), two of which are AB interface mutations (I125R and V127T), and four of which are miscellaneous surface mutations (T21S, H41T, C117T, and S131P) (38). These mutations produce a stable dimeric variant, which, being characterized by an  $\sim 15\%$  decrease in the fluorescence quantum yield, was shown to have an extinction coefficient comparable with that of DsRed1 (38). Furthermore, dimer2 was shown to acquire red fluorescence at 37 °C more than 5 times faster than DsRed1 (38).

Finally, zFP506 is a GFP-like protein isolated from *Zoanthus* sp. (7). This protein is very different from *A. victoria* GFP in its amino acid sequence (the sequences of GFP and zFP506 are  $\sim 25\%$  identical; see below), but major spectroscopic properties of GFP and zFP506 are rather similar (7). Recently, it has been shown that in contrast to the monomeric GFP from *A. victoria*, zFP506 is predominantly a tetramer (15).

## MATERIALS AND METHODS

**Plasmid Construction.** The plasmids encoding EGFP, zFP506, mRFP1, dimer2, and DsRed1 with polyhistidine tags were constructed as described previously (18) and were transfected into *Escherichia coli* BL21(DE3) (Invitrogen).

**Recombinant Proteins and Their Analysis.** The FP expression in *E. coli* was induced with 1 mM IPTG (Nacalai tesque) during 24 h at 37 °C, and proteins were purified with Ni-NTA agarose (Qiagen). The samples were at least 95% pure according to SDS-PAGE. Protein concentrations were determined by the Bio-Rad protein assay kit, and adjusted to 0.05 mg/mL in 50 mM Tris-HCl buffer (pH 8.0). For denaturation in GdmCl (Nacalai tesque), concentrations of GdmCl were determined by refraction indexes using an Abbe refractometer (LOMO).

**Fluorescence Spectroscopy.** Specific green or red fluorescence has been excited at 365 nm, and emission was detected at 510 nm for EGFP and zFP506, at 585 nm for DsRed1 and dimer2, and at 610 nm for mRFP1. The tryptophan fluorescence has been excited at 297 nm, and emission was registered at the wavelength corresponding to the maximal fluorescence intensity (uncorrected for the spectral sensitivity): 326 (dimer2), 320 (DsRed), 337 (EGFP), 334 (mRFP1) and 330 nm (zFP506). The fluorescence spectrophotometers described in ref 39 and F-2500 (Hitachi) were used for steady-state spectroscopic analysis. Measurements were performed with the sample temperature adjusted to 23 °C.

**Analysis of the Fluorescence Decay.** To analyze the decay curves, a special program was developed. The fitting routine was based on the nonlinear least-squares method. Minimization was accomplished according to Marquardt (40). P-

Terphenyl in ethanol and *N*-acetyltryptophanamide in water were used as reference compounds (41). Experimental data were analyzed using the multiexponential approach:

$$I(t) = \sum_i \alpha_i \exp(-t/\tau_i)$$

where  $\alpha_i$  and  $\tau_i$  are the amplitude and lifetime of component  $i$  ( $\sum \alpha_i = 1$ ).

*Stern–Volmer Quenching and Estimation of the Bimolecular Quenching Rates.* The conformational state of proteins was further characterized by acrylamide-induced fluorescence quenching. Samples were prepared in 50 mM Tris-HCl buffer and 150 mM NaCl (pH 7.5), and the protein concentrations were adjusted to provide an optical density at an excitation wavelength of less than 0.1. Aliquots of a 5.0 M acrylamide stock solution were consecutively added to 1 mL of protein solution to increase the acrylamide concentration. Experiments were performed using excitation at 365 nm with fluorescence emission set at 510 nm for EGFP and zFP506, at 585 nm for DsRed1 and dimer2, and at 610 nm for mRFP1. The tryptophan fluorescence has been excited at 297 nm and emission set at 326 (dimer2), 320 (DsRed), 337 (EGFP), 334 (mRFP1), and 330 nm (zFP506). Excitation and emission slit widths were 2 and 5 nm, respectively, and the fluorescence intensities were recorded for 30 s. Experiments were performed in triplicate, and the data were corrected for the dilution effects. Quenching data were plotted as the ratio of fluorescence in the absence of quencher ( $I_0$ ) to the intensity in the presence of quencher ( $I$ ) against quencher concentration. The resulting data were fit to dynamic parameters according to the Stern–Volmer equation

$$I_0/I = 1 + K_{SV}[Q]$$

where  $K_{SV}$  is the Stern–Volmer quenching constant and  $[Q]$  the quencher concentration (42). The bimolecular quenching rates,  $k_q$ , have been calculated from  $K_{SV}$  and green fluorescence lifetimes,  $\tau$ , as  $k_q = K_{SV}/\tau \text{ M}^{-1} \text{ s}^{-1}$  (41).

*Circular Dichroism Measurements.* CD spectra were obtained with an AVIV (Lakewood, NJ) 60DS spectrophotometer, using protein concentrations of  $\sim 0.25$  and 0.5 mg/mL for far- and near-UV CD measurements, respectively. Far-UV CD spectra were recorded in a cell with a path length of 0.1 mm from 250 to 190 nm with a step size of 0.5 nm, a bandwidth of 1.5 nm, and an averaging time of 10 s. Near-UV CD spectra were recorded in a cell with a path length of 1.0 cm from 650 to 250 nm with a step size of 1.0 nm, a bandwidth of 1.5 nm, and an averaging time of 10 s. For all spectra, an average of five scans were obtained. CD spectra of the appropriate buffers were recorded and subtracted from the protein spectra.

*GdmCl-Induced Equilibrium Unfolding.* Protein samples were incubated for the desired amounts of time at 25 °C in the presence of various concentrations of GdmCl. Unfolding curves were determined by monitoring the fluorescence spectra at 25 °C. The pH was checked to ensure a constant value throughout the whole transition, and the denaturant concentration was determined from refractive index measurements (43), using an Abbe-3L refractometer from Spectronic Instruments.

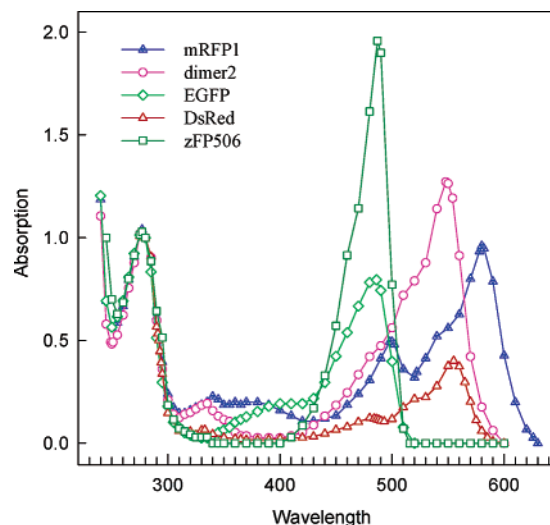


FIGURE 1: UV-vis absorbance spectra of original FPs analyzed in this study. Spectra have been normalized to have similar absorbances at 280 nm.

## RESULTS

### *Spectral Properties of Monomeric and Oligomeric Fluorescent Proteins*

The remarkable feature of GFP-like proteins is a unique chromophore, a *p*-hydroxybenzylideneimidazolidone, which is located almost at the center of the  $\beta$ -can. The chromophore consists of residues 65–67 (Ser-dehydroTyr-Gly) of the protein (GFP numbering of the amino acid residues), with the cyclized backbone of these residues forming the imidazolidone ring. Importantly, it has been noted that although the Ser-Tyr-Gly amino acid sequence could be found in different non-FPs, neither is the sequence cyclized in any of these nor the tyrosine oxidized, implying that the tendency to form such a chromophore does not represent the intrinsic property of this tripeptide, and is dependent on its specific local environment. It is well-known that the major spectroscopic characteristics of FPs (such as positions and shapes of their absorption and fluorescence spectra) are determined by the peculiarities of the local environment of the chromophore (4, 26, 44). Taking into account the fact that five proteins used in this study differ in their amino acid sequences (see above), we were not surprised that they possess very distinctive spectral properties.

*Absorbance Spectra.* Figure 1 compares absorbance spectra of EGFP (green monomer), zFP506 (green tetramer), mRFP1 (red monomer), dimer2 (red dimer), and DsRed1 (red tetramer). Note that the spectra of proteins have been normalized to show similar intensity at 280 nm. The maximal absorbance for red FPs is observed at 548, 555, and 580 nm for dimer2, DsRed1, and mRFP1, respectively. The red FPs possess rather complex absorption spectra. All of them have a short-wavelength component (an absorbance band with the maximum in the vicinity of 334 nm); DsRed1 and dimer2 have shoulders in the vicinity of 480–490 and 520 nm, whereas the spectrum of mRFP1 in addition to the shoulder at 550 nm is characterized by a new peak with a maximal absorbance in the vicinity of 500 nm. Finally, mRFP1 has an additional absorbance band at 380 nm (see Figure 1). The absorption spectra of green FPs are simpler. The spectra of EGFP and zFP506 are characterized by maximal absorbances

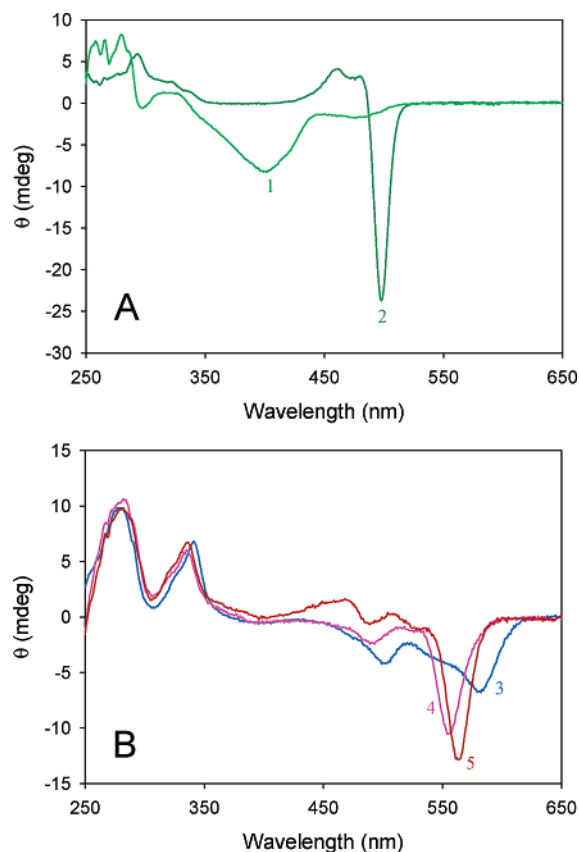


FIGURE 2: Near-UV-vis CD spectra of green (A) and red (B) fluorescent proteins: (A) EGFP (light green line, 1) and zFP506 (dark green line, 2) and (B) mRFPI (blue line, 3), dimer2 (pink line, 4), and DsRed (red line, 5).

at 486 and 487 nm, respectively; both of them have a shoulder in the vicinity of 460 nm, and EGFP has an additional shoulder at 400 nm (see Figure 1).

*Secondary and Tertiary Structures from CD Spectra.* We have established that all five proteins possess very similar secondary structures, as their far-UV CD spectra were almost indistinguishable (data not shown). On the other hand, Figure 2A shows the existence of a considerable difference for the near-UV-vis CD spectra measured for green FPs. It has previously been emphasized that all dichroic bands in the visible region of FPs have small negative Cotton effects, and are visible at the high optical density of the chromophore (45). A comparison of the data for the EGFP indicates that although the absorption band at 400 nm has a much lower oscillator strength than the one arising at 490 nm, the rotational strength of bands shows the opposite behavior (cf. Figures 1 and 2A). In agreement with the absorption spectrum, Figure 2A shows that zFP506 possesses a complete lack of the 400 nm band, and very strong negative ellipticity in the vicinity of 490 nm. Interestingly, the near-UV-vis CD spectra of red FPs are more alike, as all of them have relatively similar spectra in the near-UV region, a dichroic band in the vicinity of 340–345 nm with a positive Cotton effect, and a set of three negative bands. These negative bands are located at 490, 520, and **556** nm for DsRed1, at 490, 520, and **550** nm for dimer2, and at 500, 550, and **580** nm for mRFPI (the major peaks are in bold). Overall, comparison of Figures 1 and 2 shows that all five FPs that have been studied are characterized by the remarkable similarity of their absorbance and CD spectra in the visible region (in

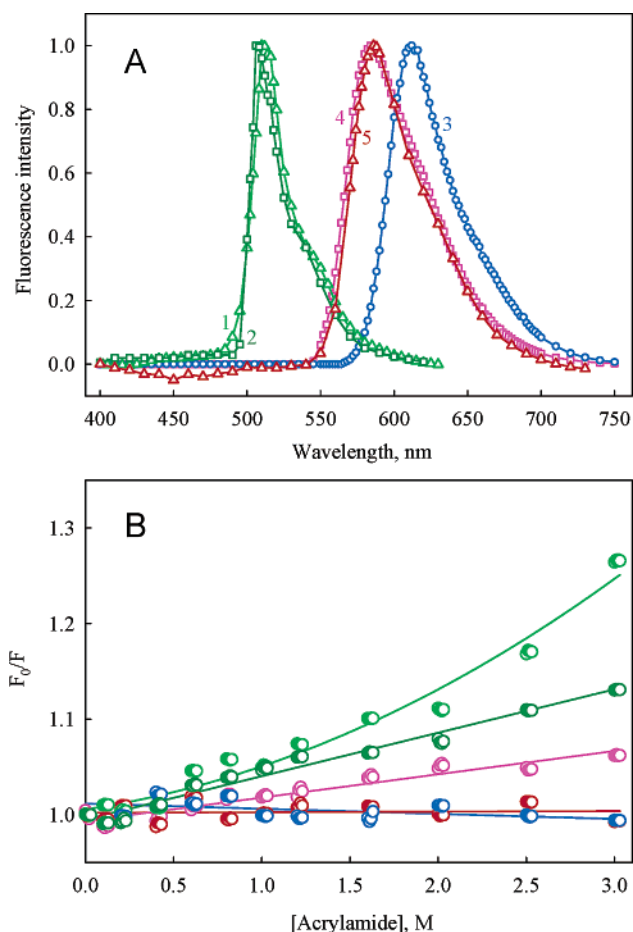


FIGURE 3: (A) Characteristic green and red fluorescence of EGFP (1), zFP506 (2), mRFPI (3), dimer2 (4), and DsRed (5). Spectra have been normalized so that they have similar maximal intensities. (B) Variations in the accessibility of the chromophore to acrylamide quenching. Stern-Volmer plots obtained from quenching studies of EGFP (light green line and symbols), zFP506 (dark green line and symbols), mRFPI (blue line and symbols), dimer2 (pink line and symbols), and DsRed (red line and symbols) fluorescence by acrylamide.

fact, all bands observed in the absorption spectra are also present in the corresponding visible CD spectra). Interestingly, Figure 2B shows that near-UV CD portions of spectra (250–320 nm) are relatively similar for red FPs, reflecting like asymmetric environments of their aromatic amino acid residues, i.e., the similarity of their rigid tertiary structures. However, Figure 2A emphasizes that the rigid tertiary structures of green FPs are different, as reflected by differences in the intensities and positions of bands in the 250–320 nm region of their near-UV CD spectra.

*Fluorescence and Solvent Accessibility of the Chromophore.* Figure 3A compares fluorescence spectra measured for EGFP, zFP506, mRFPI, dimer2, and DsRed1. Spectra have been normalized to have similar maximal intensities. It can be seen that all five proteins are characterized by the presence of specific fluorescence with  $\lambda_{\text{max}}$  values of 506, 510, 584, 586, and 612 nm for zFP506, EGFP, dimer2, DsRed1, and mRFPI, respectively. The blue-shifted maximal fluorescence of zFP506 in comparison with that of EGFP is most likely due to the difference in the solvent accessibility of chromophore, which could be more isolated from the solvent due to the zFP506 oligomerization. Similarly, the association of red FPs (dimer2 and DsRed1) might also

Table 1: Spectral Parameters of the Fluorescent Proteins Analyzed in This Study

protein	fluorescence lifetime		chromophore accessibility to acrylamide		Trp accessibility to acrylamide	
	$\tau$ (ns)	$\chi^2$	$K_{SV}$ ( $M^{-1}$ )	$k_q$ ( $\times 10^{-7} M^{-1} s^{-1}$ )	$K_{SV}$ ( $M^{-1}$ )	$k_q$ ( $\times 10^{-7} M^{-1} s^{-1}$ )
EGFP	2.78	1.0	$0.071 \pm 0.003$	$2.6 \pm 0.1$	$2.70 \pm 0.04$	$9.7 \pm 0.1$
zFP506	3.65	1.2	$0.043 \pm 0.001$	$1.17 \pm 0.03$	$0.83 \pm 0.01$	$2.29 \pm 0.04$
mRFP1	1.75	2.3	0.00	0.00	$2.09 \pm 0.02$	$11.9 \pm 0.1$
dimer2	4.00	1.6	$0.021 \pm 0.001$	$0.53 \pm 0.03$	$0.97 \pm 0.01$	$2.4 \pm 0.2$
DsRed	3.60	1.1	$0.002 \pm 0.001$	$0.05 \pm 0.04$	$0.257 \pm 0.005$	$0.71 \pm 0.01$

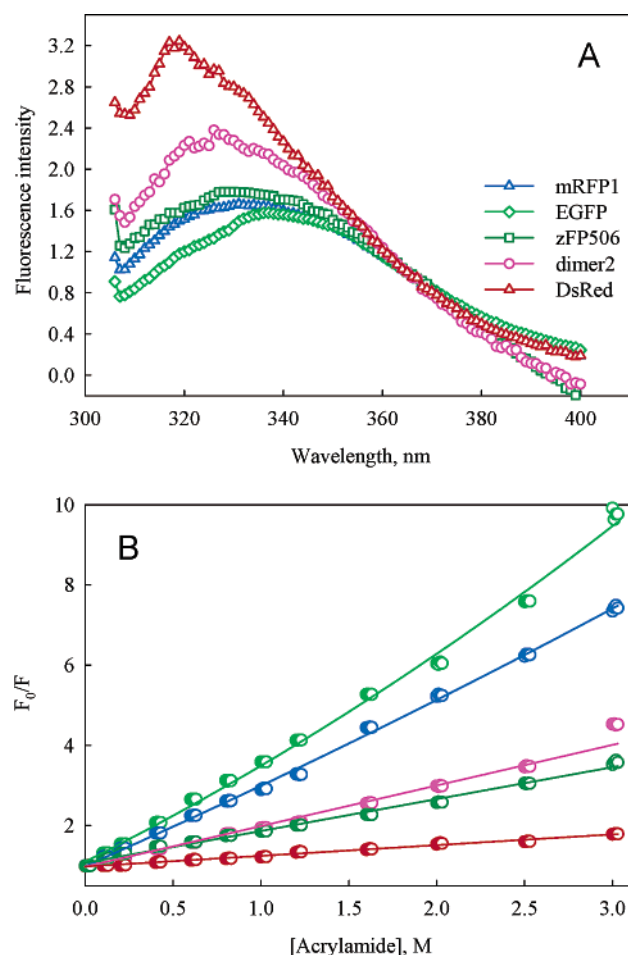


FIGURE 4: (A) Tryptophan fluorescence of EGFP (light green line and symbols), zFP506 (dark green line and symbols), mRFP1 (blue line and symbols), dimer2 (pink line and symbols), and DsRed (red line and symbols). (B) Variations in the accessibility of tryptophans to acrylamide quenching. Stern–Volmer plots obtained from quenching studies of EGFP (light green line and symbols), zFP506 (dark green line and symbols), mRFP1 (blue line and symbols), dimer2 (pink line and symbols), and DsRed (red line and symbols) fluorescence by acrylamide.

induce the enhanced protection of the chromophore from the solvent. The validity of this assumption for zFP506, EGFP, dimer2, DsRed1, and mRFP1 has been analyzed by studies of the efficiency of acrylamide quenching of their specific fluorescence. Figure 3B and Table 1 show that the chromophore is not very accessible to the quencher in all proteins, as manifested by low values of Stern–Volmer constants and slow bimolecular quenching rates (see Table 1). Interestingly, oligomerization led to the slight decrease in the values of both  $K_{SV}$  and  $k_q$  (Figure 3B and Table 1), reflecting the decreased accessibility of the chromophore to acrylamide.

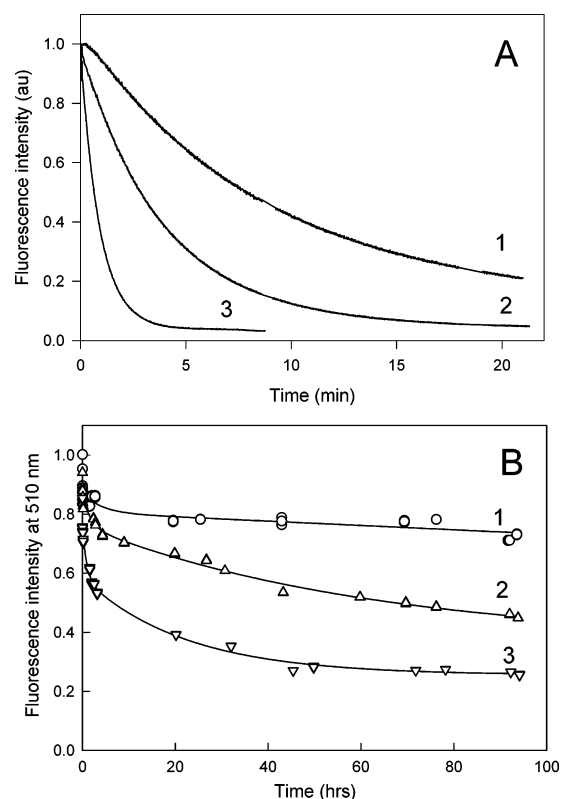


FIGURE 5: Kinetics of fluorescence changes for EGFP (A) and zFP506 (B) accompanying protein unfolding in 4.0 (1), 5.6 (2), and 6.2 M GdmCl (3).

*Peculiarities of Trp Fluorescence.* Additional information about the accessibility of the protein interior to solvent could be obtained from the analysis of Trp fluorescence. Figure 4A shows that FPs are characterized by the noticeable differences in the position of their Trp fluorescence spectra. In fact, the Trp spectrum of zFP506 is blue-shifted in comparison with that of EGFP, whereas red FPs form the following series with respect to their maximal Trp fluorescence (from longer to shorter wavelengths): mRFP1 > dimer2 > DsRed. In other words, monomeric green and red FPs are characterized by the red-shifted Trp fluorescence in comparison with their oligomeric forms, suggesting that the accessibility of Trp residues to solvent can be decreased due to FP oligomerization. This assumption was confirmed by the acrylamide quenching experiments. Figure 4B and Table 1 show that Trps are not very accessible to quencher in all proteins, as manifested by low values of Stern–Volmer constants. However, the oligomerization led to the further decrease in the accessibility of Trp to acrylamide, as it is reflected in the decreased  $K_{SV}$  values measured for zFP506, dimer2, and DsRed.

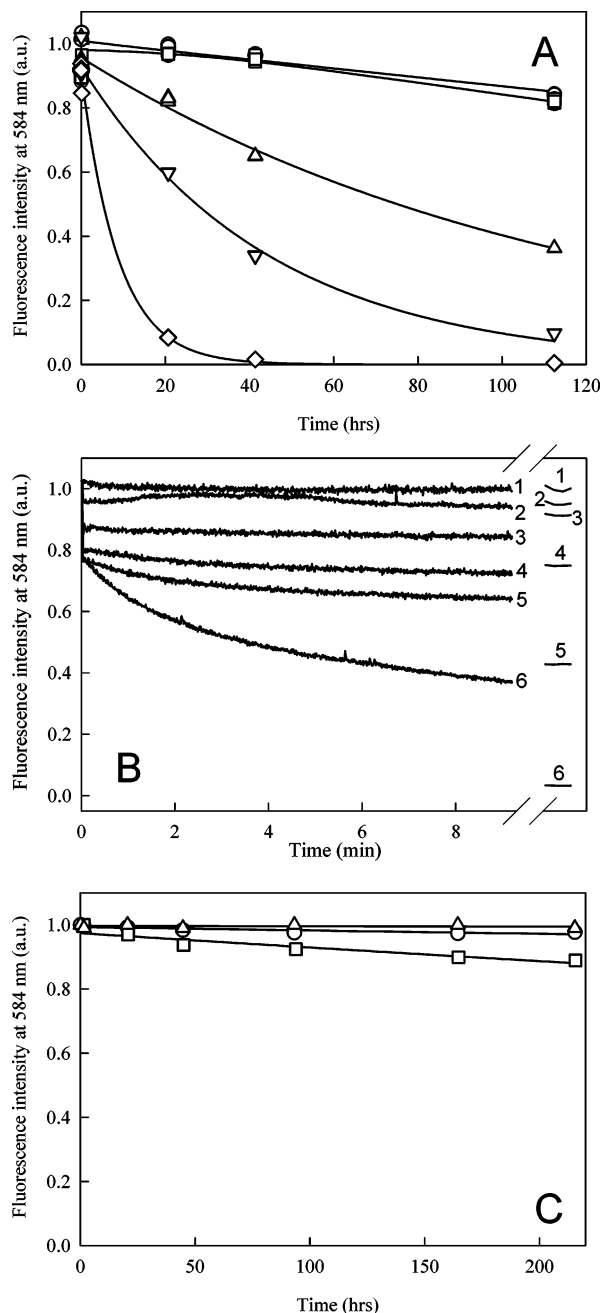


FIGURE 6: Kinetics of fluorescence changes for mRFP1 (A), dimer2 (B), and DsRed (C) accompanying protein unfolding. The final GdmCl concentrations were (A) 2 (○), 4 (□), 5.2 (△), 5.6 (▽), and 6.5 M (◇), (B) 0 (1), 0.1 (2), 2.0 (3), 4.0 (4), 5.2 (5), and 6.5 M (6), and (C) 4.0 (○), 5.6 (△), and 6.2 M GdmCl (□).

**Fluorescence Resonance Energy Transfer.** The intensity of Trp fluorescence for all FPs that have been studied is relatively low. This may be due to the fluorescence resonance energy transfer (FRET) from excited Trp to the FP chromophore. The obvious prerequisite for FRET is the spectral overlap between the donor's emission and the acceptor's absorption spectra, i.e., the overlapping of the Trp emission with the FP chromophore absorption spectra. Figure 1 shows that proteins such as mRFP1, dimer2, and EGFP definitely possess pronounced absorbance bands in the vicinity of 320–370 nm. On the other hand, the intensities of the corresponding bands for DsRed and zFP506 are essentially lower, assuming that FRET for these proteins should be less effective. However, data presented in Figure 4A are incon-

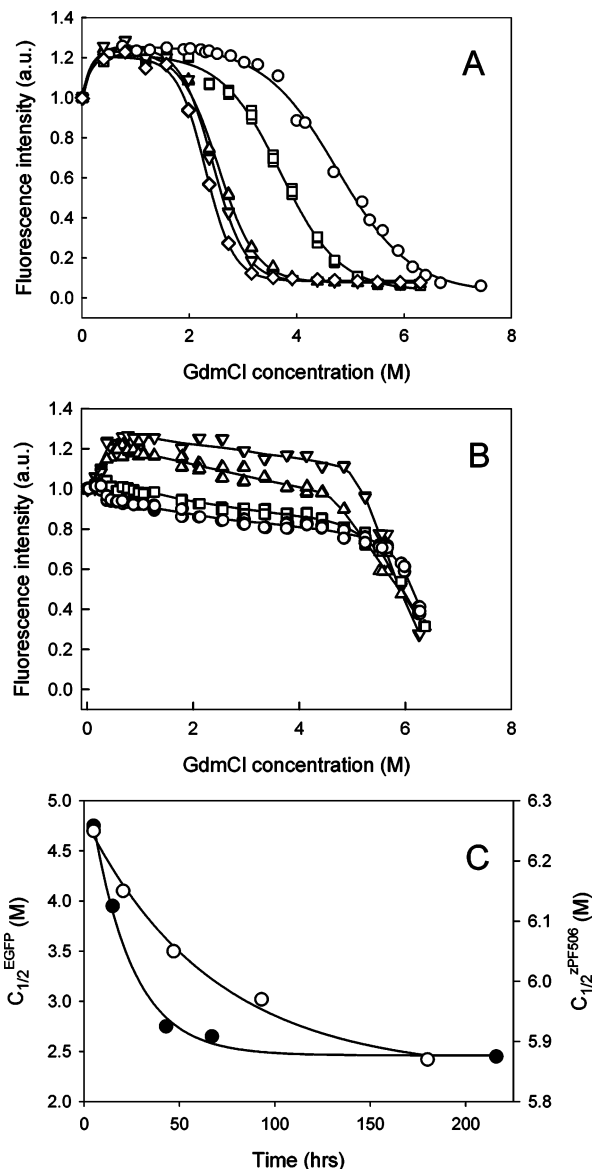


FIGURE 7: Quasi-equilibrium unfolding of EGFP (A) and zFP506 (B) induced by GdmCl. Measurements for EGFP were performed after incubation for 5 (○), 15 (□), 43 (△), 67 (▽), and 216 h (◇) in the presence of the desired GdmCl concentration. The fluorescence was excited at 365 nm and detected at 510 nm for EGFP and zFP506, at 585 nm for DsRed1 and dimer2, and at 610 nm for mRFP1. Measurements for zFP506 were taken after incubation for 1 (○), 2 (□), 3 (△), and 5 days (▽) in the presence of the desired GdmCl concentration. (C) Kinetics of the approach of the unfolding equilibrium determined as  $C_{1/2}$  vs incubation time dependencies for EGFP (●, left axis of the ordinate) and zFP506 (○, right axis of the ordinate).  $C_{1/2}$  values have been estimated from the sigmoidal fits of corresponding data sets in panels A and B.

sistent with this assumption, as Trp fluorescence of DsRed is in fact the most intensive among the FPs that have been studied, whereas the intensity of Trp fluorescence of zFP506 is rather comparable with those of mRFP1 and EGFP. Furthermore, the existence of FRET seemed to be confirmed in the experiments when the FP fluorescence was excited in the UV region (i.e., in the vicinity of the maximal Trp absorbance). In fact, we have established that besides Trp fluorescence the intensive characteristic green or red emission was observed at the excitation at 280 nm (data not shown). This can be due to FRET from Trp to the FP chromophore. However, the presence of some specific absorption bands

Table 2: Kinetic Parameters of Unfolding of Different Fluorescent Proteins at High GdmCl Concentrations

EGFP		zFP506		mRFP1		dimer2		DsRed1	
[GdmCl] (M)	$t_{1/2}$ (min)	[GdmCl] (M)	$t_{1/2}$	[GdmCl] (M)	$t_{1/2}$	[GdmCl] (M)	$t_{1/2}$	[GdmCl] (M)	$t_{1/2}$
4.0	11.2	4.2	17% (after 93 h)	4.0	16% (after 112 h)	4.0	38% (after 116 h)	4.0	18% (after 142 h)
5.6	4.96	5.6	67 h	5.6	25 h	5.2	10.0 h	5.2	15 h
6.2	1.29	6.2	4.5 h	6.5	7 h	6.5	3.4 min	6.2	5.5 h

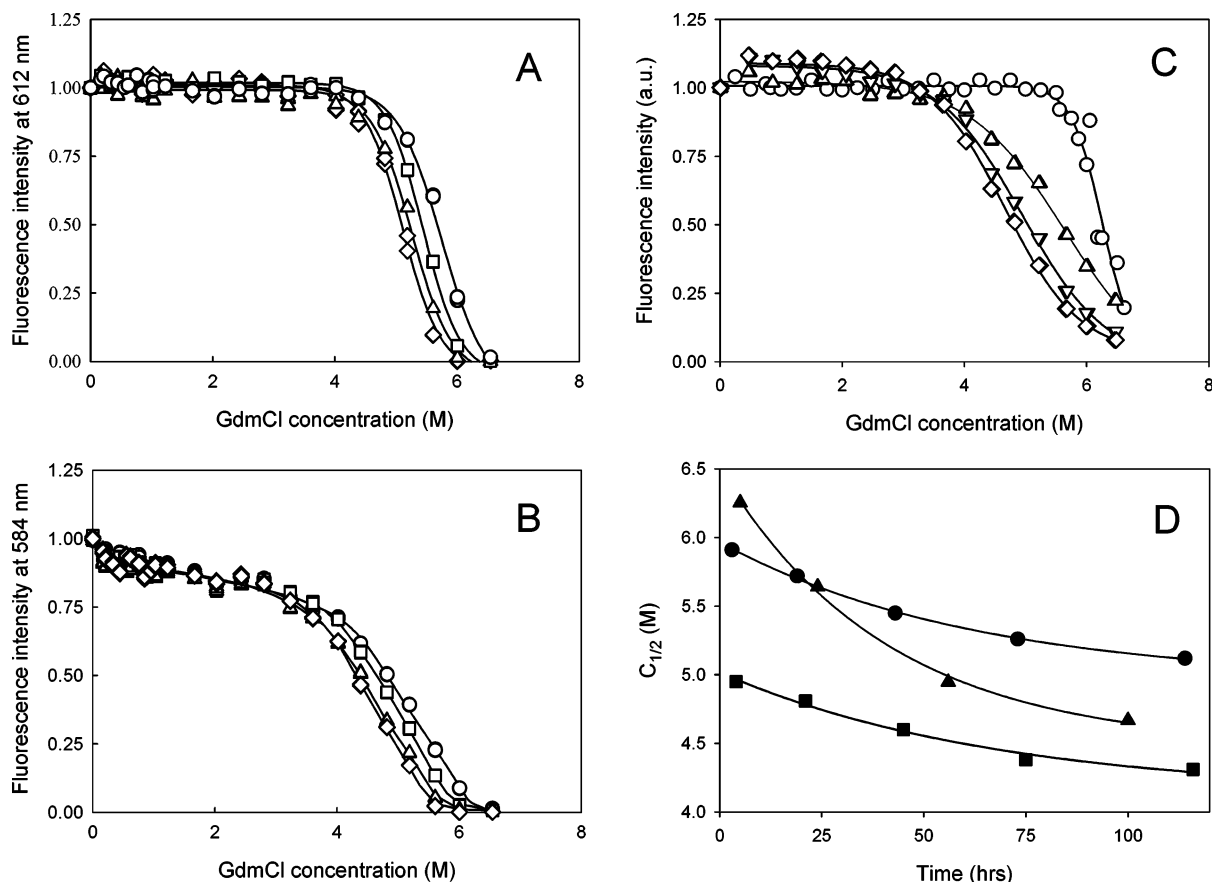


FIGURE 8: Quasi-equilibrium unfolding of mRFP1, dimer2, and DsRed induced by GdmCl. (A) Measurements for mRFP1 were taken after incubation for 1 (○), 2 (□), 3 (△), and 5 days (◇) in the presence of the desired GdmCl concentration. (B) Measurements for dimer2 were taken after incubation for 1 (○), 2 (□), 3 (△), and 5 days (◇) in the presence of the desired GdmCl concentration. Fluorescence was excited at 365 nm and detected at 510 nm for EGFP and zFP506, at 585 nm for DsRed1 and dimer2, and at 610 nm for mRFP1. (C) Measurements for DsRed were taken after incubation for 5 (○), 24 (△), 56 (▽), and 100 h (◇) in the presence of the desired GdmCl concentration. (D) Kinetics of the approach of the unfolding equilibrium determined as  $C_{1/2}$  vs incubation time dependencies for mRFP1 (●), dimer2 (■), and DsRed (▲).  $C_{1/2}$  values have been estimated from the sigmoidal fits of corresponding data sets in panels A–C.

of the FP chromophore in this region of the spectrum also cannot be excluded. All this shows that the question of FRET is still open for subsequent studies.

It is necessary to emphasize that the existence of FRET (if any) does not affect our conclusions about the Trp accessibility to the solvent and to the external quencher. In fact, FRET, being one of the nonemitting ways of the energy dissipation from the excited state, does affect the value of the quantum yield of Trp in the absence of an external quencher. On the other hand, the Stern–Volmer quenching constant,  $K_{SV}$ , and the bimolecular quenching rate constant,  $k_q$ , characterize exclusively the accessibility of the chromophore to the quencher and do not depend on other quenching processes, including FRET (42).

#### Conformational Stability of FPs

**Kinetics of GdmCl-Induced Unfolding.** Incubation of FPs in the presence of concentrated solutions of GdmCl caused

a rather slow decrease in their fluorescence intensities (see Figures 5 and 6). Figure 5A shows that in the concentrated GdmCl solutions (in the presence of 4.0, 5.6, and 6.2 M GdmCl), EGFP unfolds within minutes. The incubation of zFP506 at GdmCl concentrations below 4.5 M did not cause significant changes in the fluorescence intensity (see Figure 5B), whereas the addition of higher GdmCl concentrations induced very slow unfolding (on a time scale of several hours). Thus, these data evidence that zFP506 is dramatically more stable than EGFP, presumably due to the tetramerization.

A complementary set of data for the series of red FPs revealed different behavior. Figure 6A shows that it took hours to unfold mRFP1 with high GdmCl concentrations, whereas dimeric dimer2 was essentially less stable, as its fluorescence noticeably decreased within minutes when concentrated GdmCl was present (see Figure 6B). On the other hand, DsRed was extremely stable, as this protein lost

only ~11% of its fluorescence intensity after being incubated for more than 20 h in the presence of 6.2 M GdmCl (see Figure 6C). Thus, among three red fluorescent proteins that have been studied, dimer2 is the least stable. Kinetically, the GdmCl-induced unfolding of FPs is a monoexponential process, with the half-time decreasing with the increase in denaturant concentration. This is summarized in Table 2, which represents the kinetic data for the unfolding of FPs in the solutions with high GdmCl concentrations. Overall, these data show that fluorescent proteins form the following series with respect to their rates of GdmCl-induced unfolding (from the slowest to the fastest): DsRed < zFP506 < mRFP1 < dimer2 < EGFP.

**Establishing the Unfolding Equilibrium.** Figures 7 and 8 show that the establishment of an unfolding equilibrium is an extremely slow process for all FPs that have been studied. Here, the resistance of proteins to the GdmCl-induced unfolding is compared using changes in green (Figure 7) or red fluorescence (Figure 8), and unfolding curves in panels A and B of Figure 7 and panels A–C of Figure 8 reflect the GdmCl-induced changes in fluorescence intensity measured for a given protein (EGFP, zFP506, mRFP1, dimer2, and DsRed, respectively) after incubation for the desired amount of time in the presence of the desired GdmCl concentration. These data have been used to plot the kinetics of the approach of the unfolding equilibrium (Figures 7C and 8D), as time courses of corresponding  $C_{1/2}$  values (half-transition concentrations of GdmCl). This gave rate constants of  $(17.73 \pm 0.22) \times 10^{-6}$  and  $(4.17 \pm 0.22) \times 10^{-6} \text{ s}^{-1}$  for EGFP and zFP506, respectively (Figure 7C), and rate constants of  $(4.57 \pm 0.26) \times 10^{-6}$ ,  $(3.89 \pm 0.19) \times 10^{-6}$ , and  $(9.59 \pm 0.76) \times 10^{-6} \text{ s}^{-1}$  for mRFP1, dimer2, and DsRed, respectively. Thus, for all fluorescent proteins that have been studied here, it takes several days to approach the unfolding equilibrium, which is rather unusual. Another interesting observation is that EGFP reaches equilibrium faster than zFP506, assuming that for green FPs this process is partially controlled by association (however, even monomeric EGFP unfolds and approaches equilibrium very slowly). The process of establishing an unfolding equilibrium in red FPs seems to be much less dependent on the protein associate state.

**Equilibrium GdmCl-Induced Unfolding.** Figure 9A represents equilibrium GdmCl-induced unfolding curves for FPs and further confirms the conclusion about the dramatic difference in the conformational stability of FPs. As the establishment of the unfolding equilibrium in FPs is a very slow process (see above and ref 32), data for this plot accumulated after the incubation of all proteins in the presence of the desired GdmCl concentration for 5–6 days. Figure 9A shows that the addition of small concentrations of denaturant (0.4 M GdmCl) induces a considerable increase (~20%) in the green fluorescence intensity for both EGFP and zFP506. The fluorescence intensity remains unchanged within the intervals of 0.4–2.0 and 0.4–5.6 M GdmCl for EGFP and zFP506, respectively, and then sharply decreases. On the other hand, small concentrations of GdmCl affected red fluorescence in a different manner. We have detected a 10% increase in the fluorescence intensity of DsRed after the addition of 0.4 M GdmCl; on the other hand, the fluorescence of dimer2 decreases by 10% under the same conditions, and the red fluorescence of mRFP1 remains

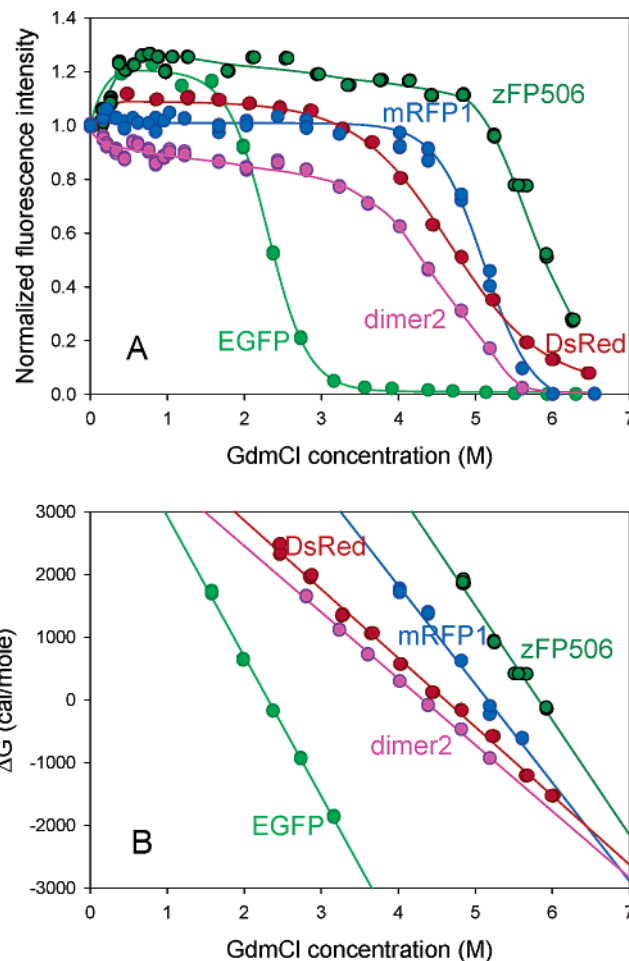


FIGURE 9: Equilibrium GdmCl-induced unfolding of EGFP (light green circles and lines), zFP506 (dark green circles and lines), mRFP1 (blue circles and lines), dimer2 (pink circles and lines), and DsRed (red circles and lines). Panel A represents GdmCl-induced changes in the characteristic green or red fluorescence measured after incubation for 9 days in the presence of the desired GdmCl concentration. Panel B represents the corresponding  $\Delta G$  vs [GdmCl] dependencies.

constant from 0 to 4.8 M GdmCl. Figure 9A shows that when GdmCl concentrations are higher than 0.5 M, the dependencies of the fluorescence intensities on denaturant concentrations are typical sigmoidal curves.

The data presented in Figure 9A can be used for the thermodynamic analysis in the assumption that fluorescent proteins that have been studied unfold by a two-state mechanism. In fact, these data could be used to calculate the dependence of the standard free energy of denaturation,  $\Delta G^\circ (= -RT \ln K)$ , on GdmCl concentration. Here  $R$  is the gas constant,  $T$  the absolute temperature, and  $K$  the equilibrium constant, which can be calculated from the experimental data by using the standard equation (46):

$$K = [(y)_N - (y)] / [(y) - (y)_D]$$

where  $(y)$  is the observed value of the parameter used to follow unfolding, and  $(y)_N$  and  $(y)_D$  are the  $(y)$  values for the native state and the denatured state, respectively, under the same conditions under which  $(y)$  was measured. Results of this analysis are summarized in Figure 9B, which shows that  $\Delta G^\circ$  varies linearly with GdmCl concentration. On the

Table 3: Thermodynamic Parameters of GdmCl-Induced Unfolding of Different FPs, As Obtained from the Analysis of the Equilibrium Transitions

protein	$\Delta G(\text{H}_2\text{O})$ (kcal/mol)	$m$ (kcal mol <sup>-1</sup> M <sup>-1</sup> )	$C_{1/2}$ (M)
EGFP	5.16 ± 0.54	2.23 ± 0.18	2.32
zFP506	10.63 ± 0.84	1.83 ± 0.20	5.87
mRFP1	8.10 ± 0.68	1.57 ± 0.17	4.95
dimer2	4.57 ± 0.42	1.06 ± 0.11	4.12
DsRed1	5.06 ± 0.49	1.11 ± 0.12	4.48

basis of these results, the conformational stability of FPs has been estimated using the equation (43)

$$\Delta G^\circ = \Delta G(\text{H}_2\text{O}) - m[\text{GdmCl}]$$

where  $\Delta G(\text{H}_2\text{O})$  is an estimate of the conformational stability of a protein that assumes that the linear dependence continues to 0 M denaturant and  $m$  is a measure of the dependence of  $\Delta G$  on GdmCl concentration, i.e., the slope of the corresponding plot. Results of this analysis for equilibrium unfolding of different FPs, together with the corresponding  $C_{1/2}$  values (midpoints of the unfolding curves), are shown in Table 3. It can be seen that zFP506 is much more stable than EGFP, whereas according to their conformational stability, red FPs are distributed as follows: dimer2 < DsRed < mRFP1.

## DISCUSSION

Previously, it has been shown that EGFP and DsRed possess a dramatic difference in their conformational stabilities both *in vitro* and *in vivo* (33). In fact, it has been established that both these proteins possess unusually slow kinetics of the approach of the unfolding equilibrium; it took 3 and 6 days for EGFP and DsRed, respectively, to reach

the quasi-equilibrium unfolding conditions, where DsRed was essentially more stable than EGFP. DsRed was shown to unfold considerably slower than EGFP both under the action of high temperatures and high GdmCl concentrations. Finally, the DsRed lifetime in cultured cells and in embryos was shown to be several times longer than that of EGFP (33).

It has been pointed out that the high degree of homology in packing of internal residues in EGFP and DsRed cannot explain the outstanding stability of the latter, and the remarkable conformational stability of DsRed under all the conditions that have been studied has been attributed to its tetrameric organization. In fact, the analysis of the DsRed crystal structure revealed that each monomer of DsRed buries 10.4 and 13.6 nm<sup>2</sup> in the interfaces due to tetramer formation, with the former having a highly hydrophobic organization that involves tight packing of 20 residues (14, 15). Furthermore, the tight packing of C-termini in hydrophobic pockets of the neighboring  $\beta$ -barrels might further stabilize the DsRed tetramer. Thus, this specific packing of monomers within the oligomer might explain the high stability of the DsRed tetramer. It has been shown that GFP-like proteins from other *Anthozoa* organisms with obligate dimeric organization also exhibited higher resistance against unfolding. *Renilla reniformis* GFP was shown to lose its fluorescence in detergents significantly more slowly than *Aequorea* GFP (19), and *Renilla muelleri* GFP had a melting temperature higher than that of EGFP (31).

In this study, we have undertaken a systematic analysis of series of green and red fluorescent proteins with different association states in an effort to understand the general role of quaternary structure in the conformational stability of fluorescent proteins. Overall, our data revealed that conformational stabilities of fluorescent proteins varied dramati-

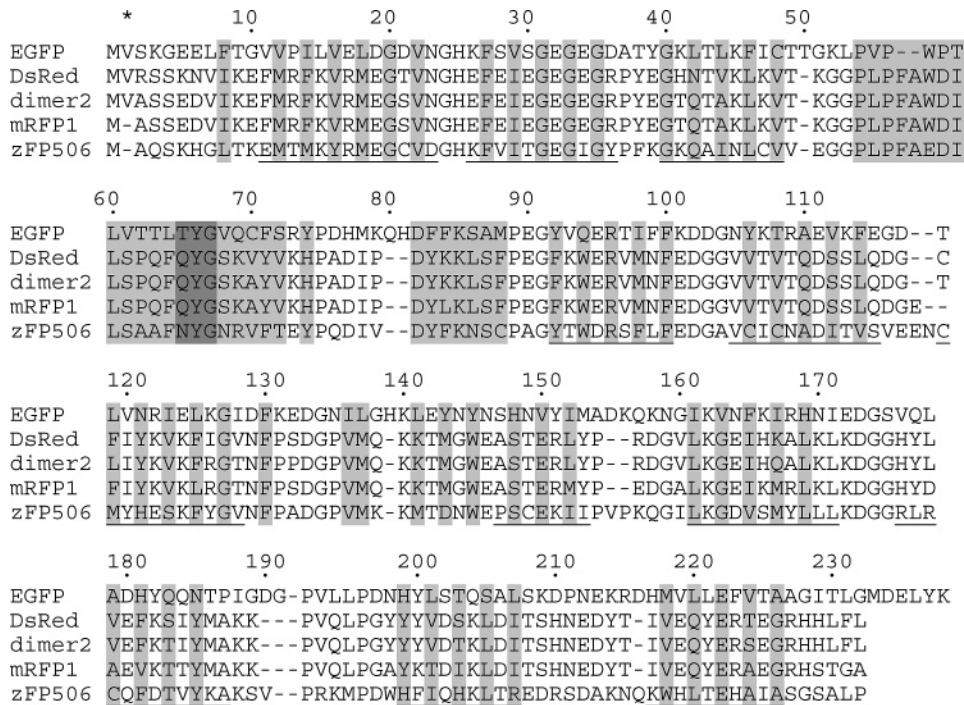


FIGURE 10: Sequence alignment of GFP-like proteins that have been studied. Polypeptide sequences for the *A. victoria* EGFP variant, *Discosoma* sp. DsRed, dimeric and monomeric mutants of DsRed, dimer2, and mRFP1, respectively, and *Zoanthus* sp. zFP506 are shown. Buried residues are highlighted in light gray, and residues 65–67 which are responsible for the chromophore synthesis are highlighted in dark gray.  $\beta$ -Sheet-forming regions are underlined. The asterisk denotes the residue, Val1A, added to EGFP, DsRed, and dimer2 genes and present in the recombinant proteins. The numbering is based on that of EGFP.

Table 4: Levels of Sequence Identity between the Pairs of the GFP-like Proteins that Have Been Studied<sup>a</sup>

protein	EGFP	DsRed	dimer2	mRFP1	zFP506
EGFP	100%	24.2%	25.6%	25.3%	23.9%
DsRed	24.2%	100%	92.4%	86.9%	43.6%
dimer2	25.6%	92.4%	100%	91.0%	43.2%
mRFP1	25.3%	86.9%	91.0%	100%	43.1%
zFP506	23.9%	43.6%	43.2%	43.1%	100%

<sup>a</sup> The residue Val1A present in EGFP, DsRed, and dimer2 was removed for the calculations.

cally. In series of green FPs, protein association could in fact be considered an important stabilizing factor, as tetrameric zFP506 was shown to be much more stable than monomeric EGFP. This was manifested by its more than 2.5-fold higher equilibrium  $C_{1/2}$  value (5.9 M GdmCl vs 2.3 M GdmCl), the 2-fold increase in conformational stability,  $\Delta G(H_2O)$ , and the dramatic increase in the time required to reach the unfolding equilibrium (see Figures 7 and 9 and Table 3). We understand that the direct comparison of EGFP and zFP506 is not straightforward, as the sequences of these proteins are only 23.9% identical (see Figure 10 and Table 4). Furthermore, the lack of the crystal structure for zFP506 makes it impossible to reveal any peculiarities of the polypeptide chain packing within the tetrameric structure. This means that there is no obvious way to control the effect of factors other than oligomerization state, and the study seems to be bound to remain inconclusive unless hundreds of proteins of various colors, evolutionary origins, and oligomerization states would be available for analysis to determine statistically whether there is any trend in the effect of the oligomerization state on the conformational stability of a given FP. However, as zFP506 was shown to be the most stable FP analyzed in this study and as there is usually a high degree of homology in packing of internal residues in different FPs, we still assume here that the tetrameric organization might dramatically stabilize this protein [as in DsRed (33)].

On the other hand, our data for red FPs do not confirm this conclusion. In fact, these proteins, having relatively similar amino acid sequences (see Figure 10 and Table 4), possess surprisingly similar conformational stabilities, with monomeric mRFP1 being the most stable red FP species under the equilibrium conditions, and with tetrameric DsRed showing the slowest unfolding kinetics. These observations, together with the very fast maturation of mRFP1, which was shown to acquire red fluorescence more than 10 times faster than DsRed1 (38), allow one to consider mRFP1 an outstanding stand-alone fluorescent marker and a fusion partner for the red fluorescent bioimaging of single molecules, intact organelles, live cells, and whole organisms.

Furthermore, we are showing here that there is a dramatic difference in the conformational stabilities and unfolding kinetic parameters within the pair of green and red monomers (EGFP and mRFP1) and the pair of green and red tetramers (zFP506 and DsRed). Interestingly, monomeric EGFP is shown to be considerably less stable than monomeric mRFP1, whereas tetrameric zFP506 is the most stable species analyzed in this study (see Table 3 and Figure 9). Overall, our findings suggest the quaternary structure, being important, does not represent the only factor determining the dramatic variations between fluorescent proteins in their

conformational stabilities. This is especially obvious for the series of red FPs, where the monomeric mRFP1 was shown to be the most stable species. Importantly, like dimer2, the monomeric and highly stable mRFP1 is a result of artificial evolution, comprising the coupled site-directed and random mutagenesis of DsRed. This emphasizes that the FP conformational stability can be dramatically increased within the monomeric state as a result of the properly designed amino acid substitutions and does not require the obligatory oligomerization. This observation is very important for the future developments of new fluorescent biomarkers.

## ACKNOWLEDGMENT

We thank Alexey Uversky for careful reading and editing of the manuscript.

## REFERENCES

- Wouters, F. S., Verveer, P. J., and Bastiaens, P. I. H. (2001) Imaging biochemistry inside cells, *Trends Cell Biol.* 11, 203–211.
- Prasher, D. C., Eckenrode, V. K., Ward, W. W., Prendergast, F. G., and Cormier, M. J. (1992) Primary structure of the *Aequorea-Victoria* green-fluorescent protein, *Gene* 111, 229–233.
- Delagrave, S., Hawtin, R. E., Silva, C. M., Yang, M. M., and Youvan, D. C. (1995) Red-shifted excitation mutants of the green fluorescent protein, *Bio/Technology* 13, 151–154.
- Heim, R., Prasher, D. C., and Tsien, R. Y. (1994) Wavelength mutations and posttranslational autoxidation of green fluorescent protein, *Proc. Natl. Acad. Sci. U.S.A.* 91, 12501–12504.
- Hein, R., and Tsien, R. Y. (1996) Engineering green fluorescent protein for improved brightness, longer wavelengths and fluorescence resonance energy transfer, *Curr. Biol.* 6, 178–182.
- Ormo, M., Cubitt, A. B., Kallio, K., Gross, L. A., Tsien, R. Y., and Remington, S. J. (1996) Crystal structure of the *Aequorea victoria* green fluorescent protein, *Science* 273, 1392–1395.
- Matz, M. V., Fradkov, A. F., Labas, Y. A., Savitsky, A. P., Zaraisky, A. G., Markelov, M. L., and Lukyanov, S. A. (1999) Fluorescent proteins from nonbioluminescent *Anthozoa* species, *Nat. Biotechnol.* 17, 969–973.
- Fradkov, A. F., Chen, Y., Ding, L., Barsova, E. V., Matz, M. V., and Lukyanov, S. A. (2000) Novel fluorescent protein from *Discosoma* coral and its mutants possesses a unique far-red fluorescence, *FEBS Lett.* 479, 127–130.
- Wiedenmann, J., Elke, C., Spindler, K. D., and Funke, W. (2000) Cracks in the  $\beta$ -can: fluorescent proteins from *Anemonia sulcata* (*Anthozoa, Actinaria*), *Proc. Natl. Acad. Sci. U.S.A.* 97, 14091–14096.
- Labas, Y. A., Gurskaya, N. G., Yanushevich, Y. G., Fradkov, A. F., Lukyanov, K. A., Lukyanov, S. A., and Matz, M. V. (2002) Diversity and evolution of the green fluorescent protein family, *Proc. Natl. Acad. Sci. U.S.A.* 99, 4256–4261.
- Lukyanov, K. A., Fradkov, A. F., Gurskaya, N. G., Matz, M. V., Labas, Y. A., Savitsky, A. P., Markelov, M. L., Zaraisky, A. G., Zhao, X. N., Fang, Y., Tan, W. Y., and Lukyanov, S. A. (2000) Natural animal coloration can be determined by a nonfluorescent green fluorescent protein homolog, *J. Biol. Chem.* 275, 25879–25882.
- Gurskaya, N. G., Fradkov, A. F., Terskikh, A., Matz, M. V., Labas, Y. A., Martynov, V. I., Yanushevich, Y. G., Lukyanov, K. A., and Lukyanov, S. A. (2001) GFP-like chromoproteins as a source of far-red fluorescent proteins, *FEBS Lett.* 507, 16–20.
- Gurskaya, N. G., Savitsky, A. P., Yanushevich, Y. G., Lukyanov, S. A., and Lukyanov, K. A. (2001) Color transitions in coral's fluorescent proteins by site-directed mutagenesis, *BMC Biochem.* 2, 6.
- Terskikh, A., Fradkov, A., Ermakova, G., Zaraisky, A., Tan, P., Kajava, A. V., Zhao, X. N., Lukyanov, S., Matz, M., Kim, S., Weissman, I., and Siebert, P. (2000) "Fluorescent timer": Protein that changes color with time, *Science* 290, 1585–1588.
- Yanushevich, Y. G., Staroverov, D. B., Savitsky, A. P., Fradkov, A. F., Gurskaya, N. G., Bulina, M. E., Lukyanov, K. A., and

- Lukyanov, S. A. (2002) A strategy for the generation of non-aggregating mutants of *Anthozoa* fluorescent proteins, *FEBS Lett.* 511, 11–14.
16. Bevis, B. J., and Glick, B. S. (2002) Rapidly maturing variants of the *Discosoma* red fluorescent protein (DsRed), *Nat. Biotechnol.* 20, 83–87.
17. Lauf, U., Lopez, P., and Falk, M. M. (2001) Expression of fluorescently tagged connexins: a novel approach to rescue function of oligomeric DsRed-tagged proteins, *FEBS Lett.* 498, 11–15.
18. Verkhusha, V. V., Otsuna, H., Awasaki, T., Oda, H., Tsukita, S., and Ito, K. (2001) An enhanced mutant of red fluorescent protein DsRed for double labeling and developmental timer of neural fiber bundle formation, *J. Biol. Chem.* 276, 29621–29624.
19. Mizuno, H., Sawano, A., Eli, P., Hama, H., and Miyawaki, A. (2001) Red fluorescent protein from *Discosoma* as a fusion tag and a partner for fluorescence resonance energy transfer, *Biochemistry* 40, 2502–2510.
20. Shagin, D. A., Barsova, E. V., Yanushevich, Y. G., Fradkov, A. F., Lukyanov, K. A., Labas, Y. A., Semenova, T. N., Ugalde, J. A., Meyers, A., Nunez, J. M., Widder, E. A., Lukyanov, S. A., and Matz, M. V. (2004) GFP-like proteins as ubiquitous metazoan superfamily: evolution of functional features and structural complexity, *Mol. Biol. Evol.* 21, 841–850.
21. Tsien, R. Y. (1998) The green fluorescent protein, *Annu. Rev. Biochem.* 67, 509–544.
22. Wachter, R. M., Elsliger, M. A., Kallio, K., Hanson, G. T., and Remington, S. J. (1998) Structural basis of spectral shifts in the yellow-emission variants of green fluorescent protein, *Struct. Folding Des.* 6, 1267–1277.
23. Yang, F., Moss, L. G., and Phillips, G. N. (1996) The molecular structure of green fluorescent protein, *Nat. Biotechnol.* 14, 1246–1251.
24. Inouye, S., and Tsuji, F. I. (1994) *Aequorea* green fluorescent protein. Expression of the gene and fluorescence characteristics of the recombinant protein, *FEBS Lett.* 341, 277–280.
25. Stearns, T. (1995) Green fluorescent protein. The green revolution, *Curr. Biol.* 5, 262–264.
26. Heim, R., Cubitt, A. B., and Tsien, R. Y. (1995) Improved Green Fluorescence, *Nature* 373, 663–664.
27. Haas, J., Park, E. C., and Seed, B. (1996) Codon usage limitation in the expression of HIV-1 envelope glycoprotein, *Curr. Biol.* 6, 315–324.
28. Cormack, B. P., Valdivia, R. H., and Falkow, S. (1996) FACS-optimized mutants of the green fluorescent protein (GFP), *Gene* 173, 33–38.
29. Bokman, S. H., and Ward, W. W. (1981) Renaturation of *Aequorea* Green-Fluorescent Protein, *Biochem. Biophys. Res. Commun.* 101, 1372–1380.
30. Ward, W. W., and Bokman, S. H. (1982) Reversible Denaturation of *Aequorea* Green-Fluorescent Protein: Physical Separation and Characterization of the Renatured Protein, *Biochemistry* 21, 4535–4540.
31. Chalfie, M., Tu, Y., Euskirchen, G., Ward, W. W., and Prasher, D. C. (1994) Green Fluorescent Protein As A Marker for Gene Expression, *Science* 263, 802–805.
32. Fukuda, H., Arai, M., and Kuwajima, K. (2000) Folding of green fluorescent protein and the cycle3 mutant, *Biochemistry* 39, 12025–12032.
33. Verkhusha, V. V., Kuznetsova, I. M., Stepanenko, O. V., Zaraisky, A. G., Shavlovsky, M. M., Turoverov, K. K., and Uversky, V. N. (2003) High stability of *Discosoma* DsRed as compared to *Aequorea* EGFP, *Biochemistry* 42, 7879–7884.
34. Ward, W. W., Prentice, H. J., Roth, A. F., Cody, C. W., and Reeves, S. C. (1982) Spectral Perturbations of the *Aequorea* Green-Fluorescent Protein, *Photochem. Photobiol.* 35, 803–808.
35. Yarbrough, D., Wachter, R. M., Kallio, K., Matz, M. V., and Remington, S. J. (2001) Refined crystal structure of DsRed, a red fluorescent protein from coral, at 2.0 Å resolution, *Proc. Natl. Acad. Sci. U.S.A.* 98, 462–467.
36. Vrzheschch, P. V., Akovbian, N. A., Varfolomeyev, S. D., and Kuznetsova, V. V. (2000) Denaturation and partial renaturation of a tightly tetramerized DsRed protein under mildly acidic conditions, *FEBS Lett.* 487, 203–208.
37. Baird, G. S., Zacharias, D. A., and Tsien, R. Y. (2000) Biochemistry, mutagenesis, and oligomerization of DsRed, a red fluorescent protein from coral, *Proc. Natl. Acad. Sci. U.S.A.* 97, 11984–11989.
38. Campbell, R. E., Tour, O., Palmer, A. E., Steinbach, P. A., Baird, G. S., Zacharias, D. A., and Tsien, R. Y. (2002) A monomeric red fluorescent protein, *Proc. Natl. Acad. Sci. U.S.A.* 99, 7877–7882.
39. Turoverov, K. K., Biktashev, A. G., Dorofeiuk, A. V., and Kuznetsova, I. M. (1998) A complex of apparatus and programs for the measurement of spectral, polarization and kinetic characteristics of fluorescence in solution, *Tsitologiya* 40, 806–817.
40. Marquardt, D. W. (1963) An algorithm for least-squares estimation of nonlinear parameters. *J. Soc. Ind. Appl. Math.* 11(2), 431–441.
41. Zuker, M., Szabo, A. G., Bramall, L., Krajcarski, D. T., and Selinger, B. (1985) Delta-function convolution method (DFCM) for fluorescence decay experiments, *Rev. Sci. Instrum.* 56, 14–22.
42. Lakowicz, J. R. (1983) *Principles of Fluorescence Spectroscopy*, Plenum Press, New York.
43. Pace, C. N. (1986) Determination and analysis of urea and guanidine hydrochloride denaturation curves, *Methods Enzymol.* 131, 266–280.
44. Cubitt, A. B., Heim, R., Adams, S. R., Boyd, A. E., Gross, L. A., and Tsien, R. Y. (1995) Understanding, Improving and Using Green Fluorescent Proteins, *Trends Biochem. Sci.* 20, 448–455.
45. Visser, N. V., Hink, M. A., Borst, J. W., van der Krogt, G. N., and Visser, A. J. (2002) Circular dichroism spectroscopy of fluorescent proteins, *FEBS Lett.* 521, 31–35.
46. Tanford, C. (1968) Protein denaturation, *Adv. Protein Chem.* 23, 121–282.

BI048725T